Acta Geodyn. Geomater., Vol. 5, No. 1 (149), 5-17, 2008

THE WESTERN BOHEMIA UPPERMOST CRUST RAYLEIGH WAVE TOMOGRAPHY

Petr KOLÍNSKÝ [1)]* and Johana BROKEŠOVÁ [2), 1]

[1)] *Academy of Sciences of the Czech Republic, Institute of Rock Structure and Mechanics, Department of Seismology, V Holešovičkách 41, 182 09 Prague 8, Czech Republic*
[2)] *Charles University in Prague, Faculty of Mathematics and Physics, Department of Geophysics, V Holešovičkách 2, 180 00 Prague 8, Czech Republic*
**Corresponding author's e-mail:* kolinsky@irsm.cas.cz

(*Received* July 2007*, accepted* February 2008)

ABSTRACT
We apply a traditional method of surface wave tomography as a new approach to investigate the uppermost crust velocities in the Western Bohemia region (Czech Republic). It enables us to look for velocity distribution in a small scale of tens of kilometers. We measure Rayleigh wave group velocity dispersion curves in a period range 0.25 – 2.0 s along paths crossing the region of interest. We use modified multiple-filtering method for frequency-time analysis. We compute 2-D tomography maps of group velocity distribution in the region for eight selected periods using the standard methods and programs described in literature. We discuss the velocity distribution with respect to results of former study by Nehybka and Skácelová (1997). We present a set of local dispersion curves which may be further inverted to obtain a 3-D shear wave velocity image of the area.

KEYWORDS: group velocity, frequency-time analysis, multiple filtering, Rayleigh wave tomography, Western Bohemia

INTRODUCTION

Let us present a short summary of former surveys in the region of our interest. While looking for the published papers concerning the Bohemian Massif (BM) and the Western Bohemia region (WB) especially, we may categorize them as follows:

1. SEISMICITY AND GEOLOGY

We mention the work by Fischer and Horálek (2003) with an overview of the seismic swarm occurrence. The idea of magma injection to the crust has been formulated by Špičák et al. (1999) for the WB region. These works summarize the main motivations for studying the WB region – an active area of seismic swarms is situated beneath our target region and complicated crust models were presented for the WB. Our study does not reach the depths of latter papers; however, the knowledge of uppermost parts is essential for studying the deeper crust structure.

2. REFRACTION AND REFLECTION EXPERIMENTS

In the 1960s, international deep seismic sounding profiles were performed across the BM. Data were interpreted by Beránek et al. (1973) and reinterpreted later by Novotný (1997). In 2000, the CELEBRATION (Central European Lithospheric Experiment Based on Refraction) took place (Guterch et al., 2003). Resultant 2-D models can be found in Hrubcová et al. (2005) and Růžek et al. (2007). Deep seismic sounding gave 1-D sets of block models with poor lateral resolution. Refraction experiments studied the uppermost parts of the crust. They resolved anomalies in the scale of tens of kilometers and with poor depth accuracy near the surface. We would like to present a study with refinement of the velocity structure accuracy both laterally and vertically.

3. 1-D BODY WAVE PROPAGATION

The study by Plomerová et al. (1987) presented apparent velocities of Sg and Pg waves generated by WB swarms. 1-D velocity models were given by Janský and Novotný (1997). A simple 3-D block model of the uppermost crust was published by Nehybka and Skácelová (1997). Janský et al. (2000) estimated crustal homogeneous models for four swarm subregions in WB. Málek et al. (2000) studied layered models of the upper crust of the same subregions. Novotný et al. (2004) used refraction data for uppermost crust velocity estimation. These studies provide reference models for our results. They deal with the same region of interest and concern also the uppermost crust depths of several kilometers. We choose for comparison the work by Nehybka and Skácelová (1997). The authors were the first who attempted to show the 3-D distribution of P wave

velocities in the WB region. Other detailed studies of several WB geological units may be found in Málek et al. (2004 and 2005).

4. 1-D SURFACE WAVE PROPAGATION

Wielandt et al. (1987) presented surface wave profile crossing the BM in southwest-northeast direction. Plešinger et al. (1991) gave the crustal velocity estimation for profile in southwest BM. These studies are important for the surface wave analysis methodology and as a first attempts to use surface waves for studying the BM. However, their wavelengths concern the whole crust and resolution ability is limited. Novotný (1996) compiled an average 1-D model of the WB region using surface wave studies. In this work, he concentrates on our WB area of interest, but his uppermost crust model consists of two layers only. We propose a more detailed model. Studies concerning the BM surface wave propagation and crust structure estimation were presented by Novotný et al. (1995 and 1997). These studies gave more detailed velocity distributions than Wielandt et al. (1987) and Plešinger et al. (1991), but they concern different parts of BM. Malinowski (2005) gave a structure of the uppermost crust in southwestern BM using the short-period Rayleigh waves – these waves are used in our present study. Part of his 2-D profile crosses WB. Kolínský and Málek (2007) estimated 1-D models of the crust and uppermost mantle in the southwestern BM crossing three major geological units of this area using relative phase velocity measurements of Aegean Sea earthquakes. This study was aimed for the whole crust velocity structure estimation and one of the profiles reaches WB region. This study uses waves longer than 9 s and near surface structure is not resolved well.

Kolínský and Brokešová (2007) estimated several 1-D models of WB uppermost crust v_s using short-period Love wave group velocities from quarry blasts. Our present study is a continuation of the latter paper, but as opposed to the latter work, we use Rayleigh waves for our tomography. The methodology of surface wave analysis is the same as in latter paper. We extended the amount of data and we concentrate on the same area of interest.

5. RECEIVER FUNCTIONS

Wilde-Piórko et al. (2005) published detailed v_s models under several stations in the BM obtained by the receiver function technique. Heuer et al. (2007) presented the differences between Saxothuringian and Moldanubian units in the western BM using also the receiver function technique. Geissler (2005) presented a large study of WB region using the receiver function technique as well as other geophysical exploration methods. Receiver function method gives whole crust and upper mantle structure. The uppermost crust is smoothed and not well resolved.

Our WB region surface wave tomography aims to get higher resolution of seismic velocity estimation of the region. Despite the fact that our study concerns only limited uppermost layer of the crust the results are important both for WB event localization and for understanding the seismic swarm generation since the upper crustal layers are supposed to be the most heterogeneous.

GROUP VELOCITY ANALYSIS

For the surface wave tomography, we first need to measure the group velocity dispersion. We use the method of Fourier transform-based multiple-filtering frequency-time analysis (Dziewonski et al., 1969). This is a classical technique and we have made modifications for processing signals in which the amplitudes of surface waves do not exceed the amplitudes of body waves. All the standard procedures as well as the new enhancements of the modified technique are described in details in the paper by Kolínský and Brokešová (2007). We use constant relative resolution filtering with the opportunity of controlling the width of the filters during the dispersion curve estimation. Some notes on this problem may be found in Levshin et al. (1972) and Cara (1973). The actual implementation of the parameters controlling the filtration is described in Kolínský (2004).

We use the instantaneous period computation for our filtered quasimonochromatic signals to ensure appropriate estimation of slightly varying periods along these signals. We use this procedure according to the study of Levshin et al. (1989).

We show the record envelope distribution in frequency-time plot (Fig. 1, panel A). We look for dispersion ridge representing the group velocity-period dependence (Fig. 1, panel B). Here we apply a modification of the classical technique – we do not use only the absolute amplitude values to determine the fundamental dispersion ridge, but instead, we look for all local dispersion ridges in the whole frequency-time domain (Fig. 1, panel C) and we provide a procedure for compiling the resultant dispersion curve using the combination of the local ridges (Fig. 1, panel D). The criterion of ridge continuity is used instead of criterion of highest amplitude values. Hence, we look for a ridge passing through our group velocity-period plots in the areas where we assume the fundamental mode should be present. After selecting the dispersion points, we truncate the spectrogram in the time domain to keep only the fundamental mode dispersion ridge (Fig. 1, panel E), which is used to create filtered surface wavegroup (Fig. 1, bold line in upper plot).

In case that the automatic procedure is not successful, we have the opportunity to select the dispersion ridge manually – the step from panel C to D is done by hand. Sometimes the analyst can see the dispersion ridge on a first glance in the frequency-time plots where the computer-based procedures would hardly give any reliable result.

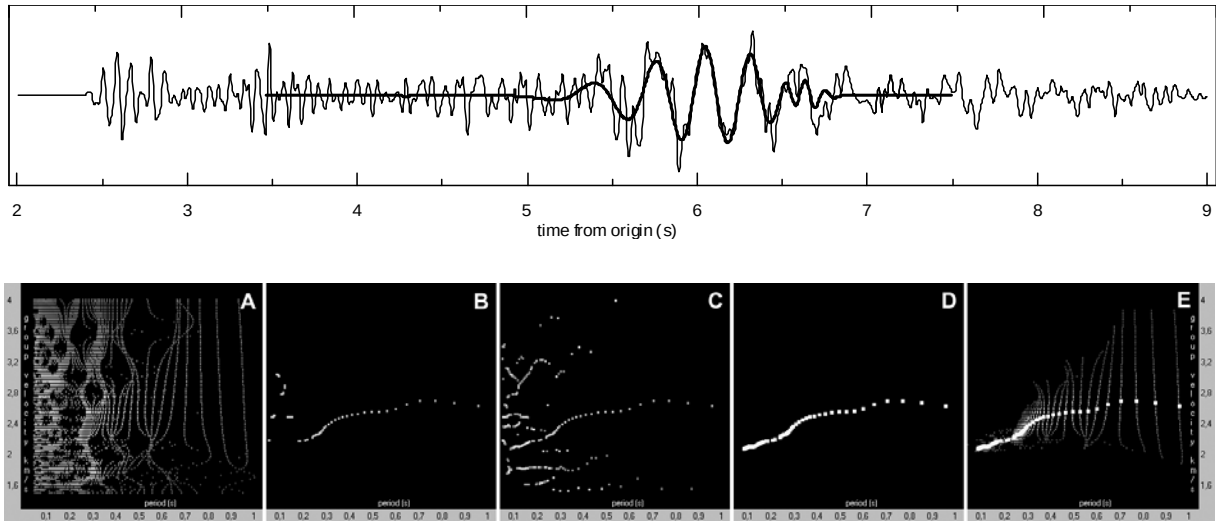

Fig. 1 Surface wave analysis example. Thin line in the upper plot represents the record from the quarry blast OTRO at the station PRAM (see Fig. 2), epicentral distance is 13.855 km and sampling frequency is 250 Hz. Bottom panels show five steps of frequency-time analysis. A: spectrogram of the record is computed. B: For each filter its absolute envelope maximum is found and plotted – we may see that only a part of the dispersion curve is formed by the arrival times of these maxima. C: All other local envelope maxima are found and plotted. D: According to the criterion of continuity the fundamental dispersion curve is compiled using all available maxima regardless of their amplitudes. E: Fundamental dispersion ridge is cut from the spectrogram along the found dispersion curve. These truncated parts of selected signals are summed to obtain the surface wavegroup as shown in upper plot by thick black line.

We use the data from the same experiment as in Kolínský and Brokešová (2007) and so the formal description of the procedures, examples and tests given in the latter work hold for this study as well. During the group velocity measurement, sets of filtered quasimonochromatic signals and filtered surface wavegroups are inspected in comparison with the raw data for each path to ensure the reliability of measurement (Fig. 1, upper plot). Different widths of filters are used for each record according to the actual properties, signal-to-noise ratio and body wave presence. Trial-and-error attitude is used for filtration parameter settings in case of complicated records to have the opportunity to choose the best resolution in both time and frequency domains in order to obtain as broad dispersion curve as possible.

GROUP VELOCITY TOMOGRAPHY

Surface wave tomography became a standard procedure for imaging the large scale heterogeneities of the Earth crust and upper mantle. We focus on local surface wave tomography study.

In the present paper we use the method described in Ditmar and Yanovskaya (1987) and Yanovskaya and Ditmar (1990). The advantage of the method is that it works also in cases when we do not have uniformly covered area with surface wave paths. The method does not use any boxes or other a priori division of the studied area. Measured velocities are entered along the ray paths and the actual velocity is given in required grid nodes. The velocity value for each grid is computed as an average of surrounding values given along the rays. In case we have only sparse ray coverage, this averaging area is larger. As it is possible to show the velocity distribution as well as the size of the averaging area, one may easily see the results with their resolving power together.

The use and further elaboration of the method is given in Yanovskaya et al. (1998), Yanovskaya et al. (2000) and Yanovskaya and Kozhevnikov (2003). This approach was successfully employed by studies dealing with regional surface wave tomography in scales smaller than continental, see for example papers by Bourova et al. (2005) (Aegean Sea) and Raykova and Nikolova (2007) (Balkan Peninsula). We use the same approach as in latter papers even for much more local problem.

Our area of interest is only 50 x 60 km and so we use the computational code, kindly provided by prof. Yanovskaya, where the area is regarded as a plane. We transform the geographical coordinates of station and blast locations to the new Cartesian coordinate system. The XY crossing zero point is located at 12.5^0 E and 50.2^0 N. The system is orientated so that at this point the Y axis is parallel to the actual meridian. Distance in the XY plane is measured in kilometers.

The tomographic procedure requires positions of each source-station pair and the velocity of propagation of the selected period of the

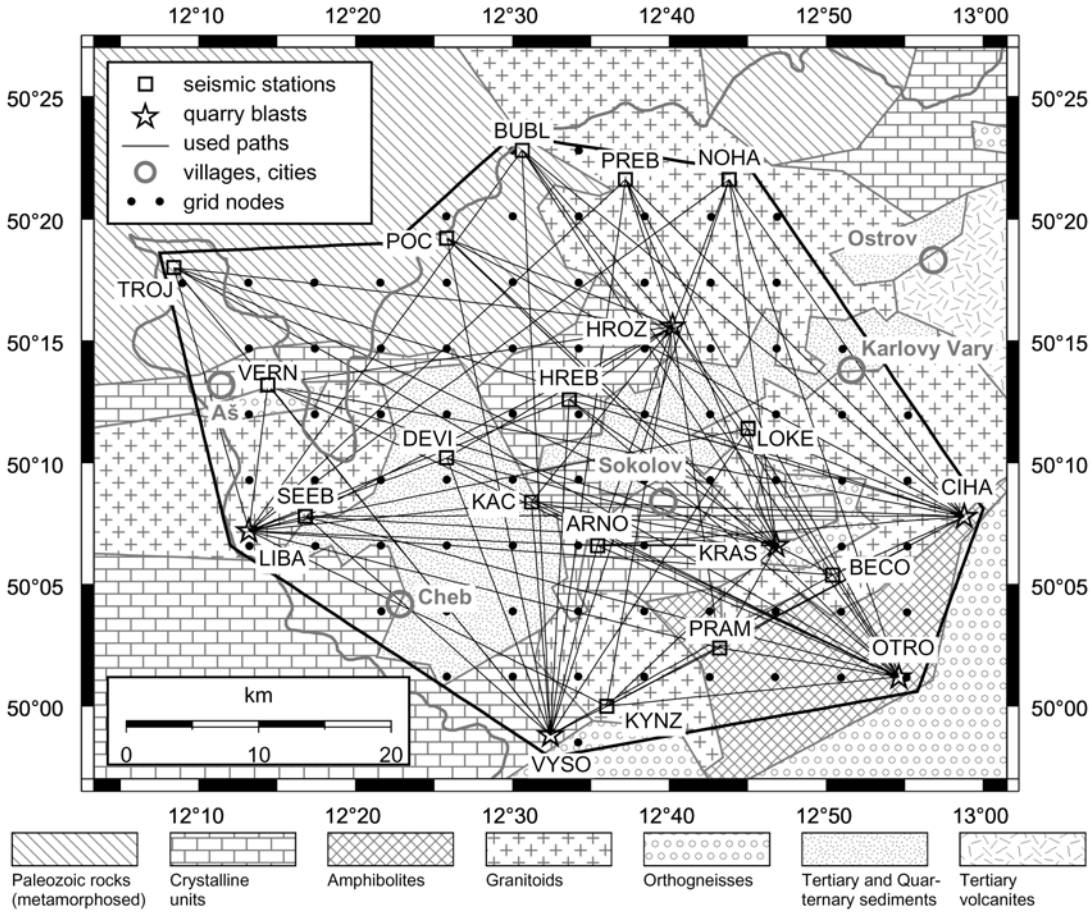

Fig. 2 Map of the Western Bohemia region. There are 15 stations (squares), 6 shot locations (stars) and 87 surface wave paths (thin solid lines) as well as several cities (gray circles) shown in the figure. Main geological units are sketched according to Mlčoch et al. (1997). Used grid nodes (dots), studied area border (bold black line) and the border between the Czech Republic and Germany (bold gray line) are shown.

corresponding dispersion curve. We may set the variance of each measured velocity and we define the positions of grid nodes where we want the resultant velocity to be estimated. As a most important tool for controlling the tomography is the regularization parameter. The higher is the value of the regularization parameter, the larger is the smoothness of the resulting velocity distribution and the larger is the averaging area for each grid node. We tested several values of the regularization parameter. Smaller value of this parameter gives very perturbed 2-D group velocity distributions. It gives smaller averaging areas and smaller residuals and hence theoretically better resolution. But it is not possible to "improve" the resolution only by using a smaller regularization parameter without considering the consequences for physical sense of the results. We choose the smoothness of the maps and hence the resolution to be comparable with wavelengths regardless of the residual improvement. This is the reason why this residual improvement is so different for different periods, as shown in Tomographic images. In the above mentioned papers we found recommended values of the regularization parameter, however, since our period range differs significantly, we used trial-and-error process to look for optimal parameter for each period.

An initial mean square travel time residual is estimated for the constant mean velocity distribution. After the tomographic procedure the remaining mean square residual is estimated. The ratio between these two residuals gives us an "improvement" of the tomography map in comparison with initial homogeneous mean velocity model.

As an output we obtain the values of velocity in required grid nodes and the size of the circular averaging area for each grid node in km. This averaging area represents the uncertainty of the tomography; as the area is smaller, the resolution of the map is better. In case of non-isotropic ray

Table 1 Coordinates, origin times and charges of the blasts.

Shot point	East longitude ^{0} WGS84	North latitude ^{0} WGS84	Altitude (m)	Charge (kg)	Date (y/m/d)	Origin time (UTC)
LIBA	12.223	50.120	590	400	2003/06/04	17:09:59.525
VYSO	12.543	49.978	700	400	2003/06/04	19:09:59.526
HROZ	12.668	50.261	560	400	2003/06/05	17:49:59.546
KRAS	12.776	50.114	740	270	2003/06/04	17:20:00.476
OTRO	12.909	50.021	605	200	2003/06/05	02:59:59.569
CIHA	12.983	50.133	730	400	2003/06/04	17:40:06.311

coverage, instead of circular averaging areas, areas elongated in the direction of rays with predominant azimuth could be considered, see Yanovskaya et al. (1998). The *rms* of each grid point is given. At the end, we transform the results back to the geographical coordinates.

DATA

Records used in the present study have been acquired during the seismic refraction experiment SUDETES 2003 (see Grad et al., 2003) which was a part of the SLICE (Seismic Lithospheric Investigation of Central Europe) international experiment. Small amount of the data have been used in the study by Kolínský and Brokešová (2007). Six shots were fired in the WB region during the experiment: Vysoká (VYSO), Číhaná (CIHA), Krásno (KRAS), Horní Rozmyšl (HROZ), Otročín (OTRO) and Libá (LIBA) and we use them in this study, see Table 1 and Fig. 2. Sixteen temporary stations were deployed in the WB region during the experiment. Data from 15 of them are used in this study; one of the stations was disturbed by some agricultural equipment. Lenartz LE-3D and Streckeisen STS-2 seismometers were used. Sampling frequency of all the stations was 250 Hz. The main purpose of this measurement was to acquire data for 3-D body wave tomography of the WB region. As a by-product of 6 blast recorded at 15 stations we have obtained 90 records containing surface waves covering an area of approximately 50 x 60 km, see Fig. 2. We use 87 of these surface wave paths in present tomography study; two of the records could not be analyzed for their low quality of signal-to-noise ratio and one of the record was discarded because it produce large arrival time residual in the whole period range.

We analyze the surface wave dispersion in a period range from 0.15 to 4.0 s, however, only few of the records produce such broad period range dispersion. This is the reason why we limit the period range from 0.25 up to 2.0 s for the tomography study.

The raw records are corrected for the instrumental response using the appropriate transfer function in the spectral domain. The velocity changes caused by the application of the transfer function are comparable with errors given by the frequency-time analysis in the given period range. However, they cause a systematic shift and so we use the corrected records for estimating the velocities to avoid this error.

The origin times of the shots have been accurately measured by a technique especially developed for this purpose. Several BR3 receivers (Brož, 2000) were installed at a distance of tens of meters from the shot to extrapolate the origin time with an accuracy of about 5 ms. For a description of the measurement method, see Málek and Žanda (2004); typical features of quarry blast records are also described there. Compared to natural earthquakes, we know the epicenter coordinates and origin times with negligible errors.

TOMOGRAPHIC IMAGES

We set grid nodes every 5 km in both directions in our Cartesian coordinate system. We clip the area of interest by an octagon corresponding to our path coverage. We present only the results for grid nodes inside of this octagon. Fig. 2 shows 79 nodes projected into geographical coordinates.

Fig. 3 presents 87 group velocity dispersion curves estimated using the dataset described in the previous section. The period values of the dispersion points are obtained using the instantaneous period estimation which is generally different for each of the curves and so we linearly interpolate the estimated group velocity values for the period values with the step of 0.05 s to have the opportunity to use the velocities of all the 87 curves at the same periods. We have decided to use the eight periods in the range from 0.25 to 2.0 s for the tomography study. Some of the curves do not cover the whole range of periods and Fig. 4 shows the number of paths for each period.

Since we do not know the group velocity variance, we set all the variances for all paths to 1.0 to give the same weight to all the data.

The averaging area, which gives us information about the resolution of the tomography maps, depends on ray coverage and on the regularization parameter controlling the smoothness of the results. We have to introduce different resolution for different wavelengths by using different regularization parameters for different periods. We set the

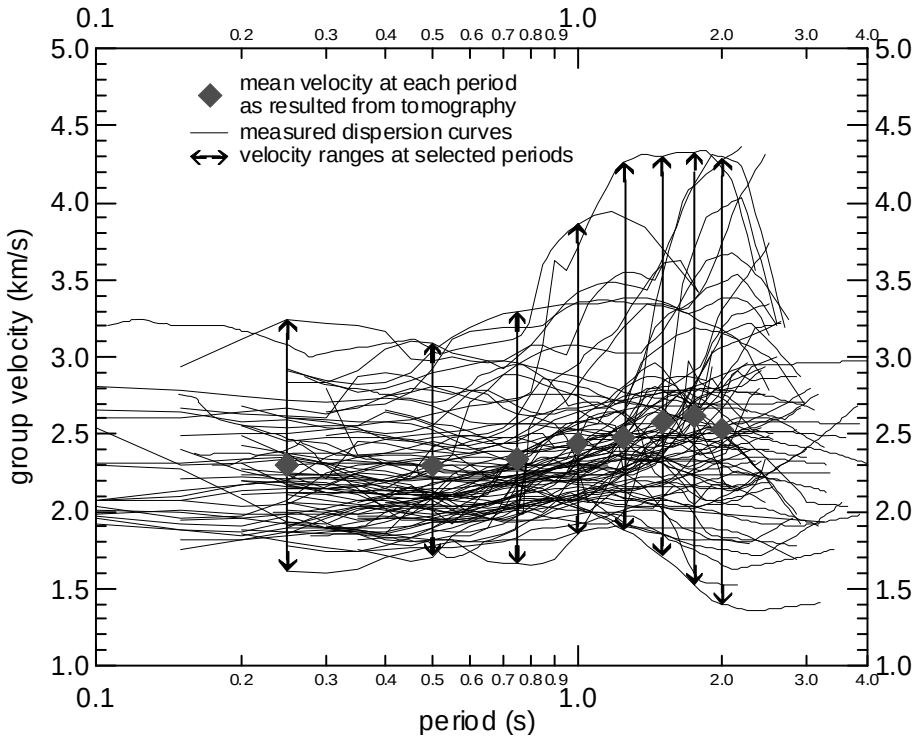

Fig. 3 Dispersion curves of Rayleigh wave group velocities measured along 87 paths (Fig. 2). Velocity ranges at eight selected periods are shown to depict the increasing velocity differences for longer waves. Values of mean velocities v_m in the studied region obtained by 2-D tomography at each period are shown by gray diamonds.

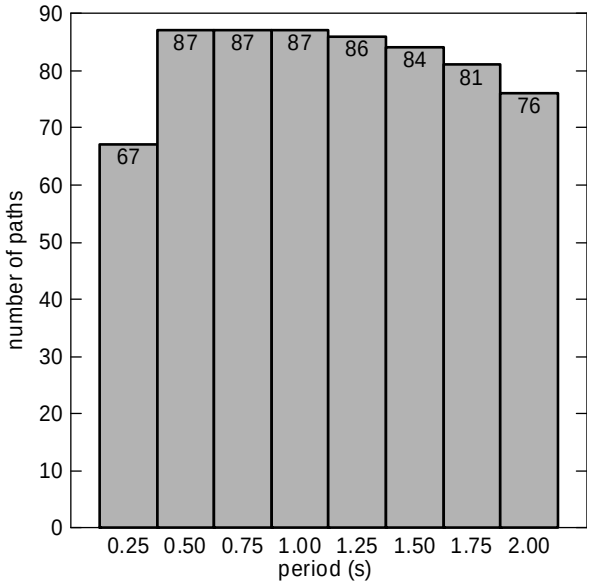

Fig. 4 Number of paths used for the tomography maps computation with respect to eight periods.

regularization parameter in such a way that for the longest period we get the smallest averaging area twice larger than corresponding wavelength. This criterion was set after many tests with different regularizations and different results. We checked the resulted maps and we choose the regularization to obtain the group velocity perturbation in reasonable range (smaller averaging area gives larger perturbations) and to obtain acceptable residual improvement (greater averaging area gives worse residual improvement). For approximate mean velocity 2.5 km/s for the period of 2.0 s the wavelength is 5.0 km. So the resolution of our longest wave is 10.0 km (radius of the averaging area is 5.0 km) and worse. In case of the shortest period we may use the same criterion, however, it has no sense to set the averaging area to be smaller than the distance of two neighboring grid nodes. If we introduced so small area, we would lose some information along parts of the paths. We set the regularization parameter so that we obtain the smallest radius of the averaging area to be 2.5 km in the best resolved grid node since our grid points are in a distance of 5.0 km. For our shortest wave of period 0.25 s and approximate mean group velocity 2.3 km/s the resolution is 4.3 times the wavelength and worse. So we obtain relatively worse resolution for shorter waves than for the longer ones in comparison to the

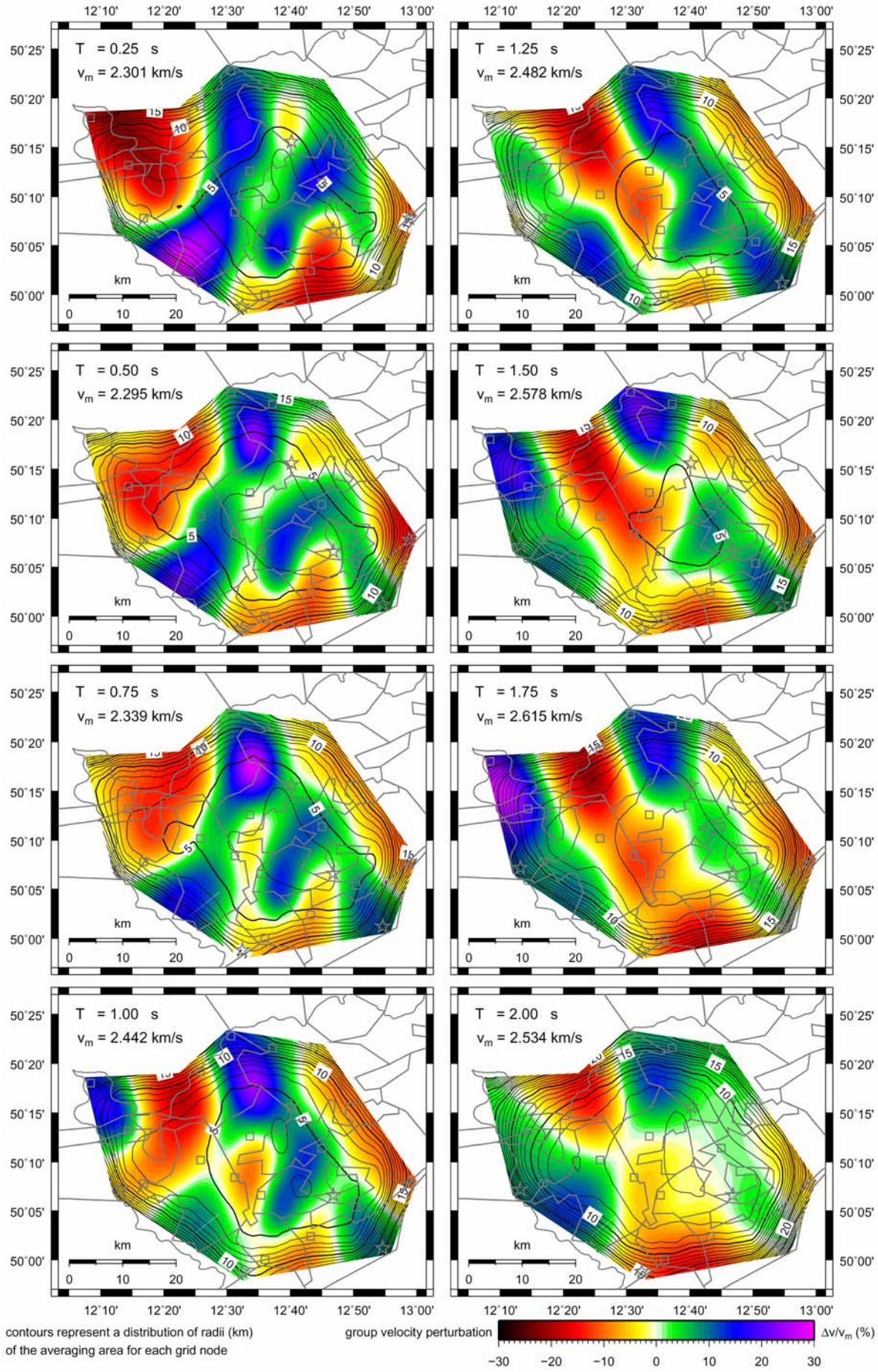

Fig. 5 2-D Rayleigh wave group velocity tomography maps of the Western Bohemia region. Each of the eight panels corresponds to the value of period *T* of the presented group velocity distribution and to the mean velocity value v_m (see Fig. 3). The color scale represents a group velocity perturbation in percent with respect to this mean velocity v_m. Isolines represent the distributions of radii of the averaging areas in kilometers.

Table 2 Number of used paths, initial and remaining residuals, improvement and mean velocities for eight selected periods.

period (s)	0.25	0.50	0.75	1.00	1.25	1.50	1.75	2.00
number of paths	67	87	87	87	86	84	81	76
initial residual (s)	1.84	1.99	1.75	1.73	1.82	1.97	2.17	2.27
remaining residual (s)	0.48	0.61	0.63	0.79	0.99	1.23	1.48	1.80
improvement (%)	74	69	64	54	46	38	32	21
mean velocity (km/s)	2.301	2.295	2.339	2.442	2.482	2.578	2.615	2.534

wavelength, but absolutely the resolution of the shortest waves is twice as good as the resolution of the longest ones.

Table 2 summarizes the number of paths (see also Fig. 4) initial and remaining travel time residuals and the resultant improvement and mean group velocities (see also Fig. 3). We see decreasing residual improvement toward longer periods. The reason is that while the initial residuals are comparable for all eight periods, due to the different regularization, which is larger for longer periods, the resulted smoother tomography maps for longer periods are able to explain smaller part of travel time residuals.

As a result, we present 2-D Rayleigh wave group velocity perturbation distributions for eight periods in the Western Bohemia region in Fig. 5. Each map is related to the mean group velocity v_m for the given period (as in Table 2 and Fig. 3) and shows the perturbation of actual group velocities to this mean value in percent. The velocity perturbations given in Fig. 5 reach up to ± 25 % in some places in case of the shorter periods.

Our ray path coverage does not prefer any azimuth considerably and so the resolution of the data is isotropic. We use the size of the averaging area for each grid node in Fig. 5 to depict this resolution. We may imagine these values as radii of circles in km of the area where the distribution of velocities using the values along the ray paths is used to estimate the resultant velocity for each grid node. These values are depicted in Fig. 5 using contours delineating the regions with the same averaging area. As the averaging area is smaller, the resolution of the tomography is better.

For comparison with Fig. 5 showing the maps for different periods, we compile the results to show the distribution of local dispersion curves around the region. Fig. 6 presents dispersion curve plots inserted into the Cartesian coordinate map. Corresponding grid nodes are to be placed in the center of each square plot. Each of the curves is compiled using eight values of group velocity of Rayleigh waves for selected eight periods in the range from 0.25 to 2.0 s. The number in each plot gives the size of the averaging area in km for period 0.5 s. Bold gray line shows the clipped region of interest as in Figs. 2 and 5. Station and blast locations with annotations are shown.

DISCUSSION AND CONCLUSION

We provide the Rayleigh wave tomography for a small region of tens of kilometers in size. It is unusual to deal with such a local problem and methodologically we may compare our results only with the works concerning larger regions. One of the parameters which help us to evaluate the results is the improvement between initial and remaining residuals. The work of Bourova et al. (2005) presents the improvement around 50 % in the Aegean Sea tomography. She uses only limited number of paths and the main criterion of her results is the smoothness of the resultant velocity distribution. The surface wave tomography of the Black Sea by Yanovskaya et al. (1998) reaches the improvement of even two thirds of the initial residual. Our results give improvement from 74 % in case of short periods down to 21 % in case of longer ones.

As we see the diversity of the dispersion curves in Fig. 3 we may assume a great heterogeneity of the studied region for the first glance, what was already shown in Kolínský and Brokešová (2007) for six of the paths. The group velocity ranges grow with the period as shown by arrows in Fig. 3 and so we may expect more pronounced 2-D velocity distribution for longer periods. The results would correspond to this assumption if we set the same regularization parameter for all eight periods, as we have tried during the tests. This approach gives the same averaging areas and hence the same resolution for all maps. In such a case the longer periods really do produce larger perturbations than the shorter ones. This is of course an approach which does not take into account the finite wavelength effect of different periods and hence a more limited resolution of longer periods.

We cannot make any conclusions whether the heterogeneity is higher near the surface or if it is more pronounced in the depth. The dispersion curve set in Fig. 3 imply for more pronounced heterogeneity in the depth but the limitation of our tomography gives us less smooth maps for shorter periods and thus higher heterogeneity for smaller depths. Generally, taking into consideration the whole Earth crust, the highest geological diversity is supposed to be at the surface. But our depth range is so limited that we may encounter higher velocity variations in the greater

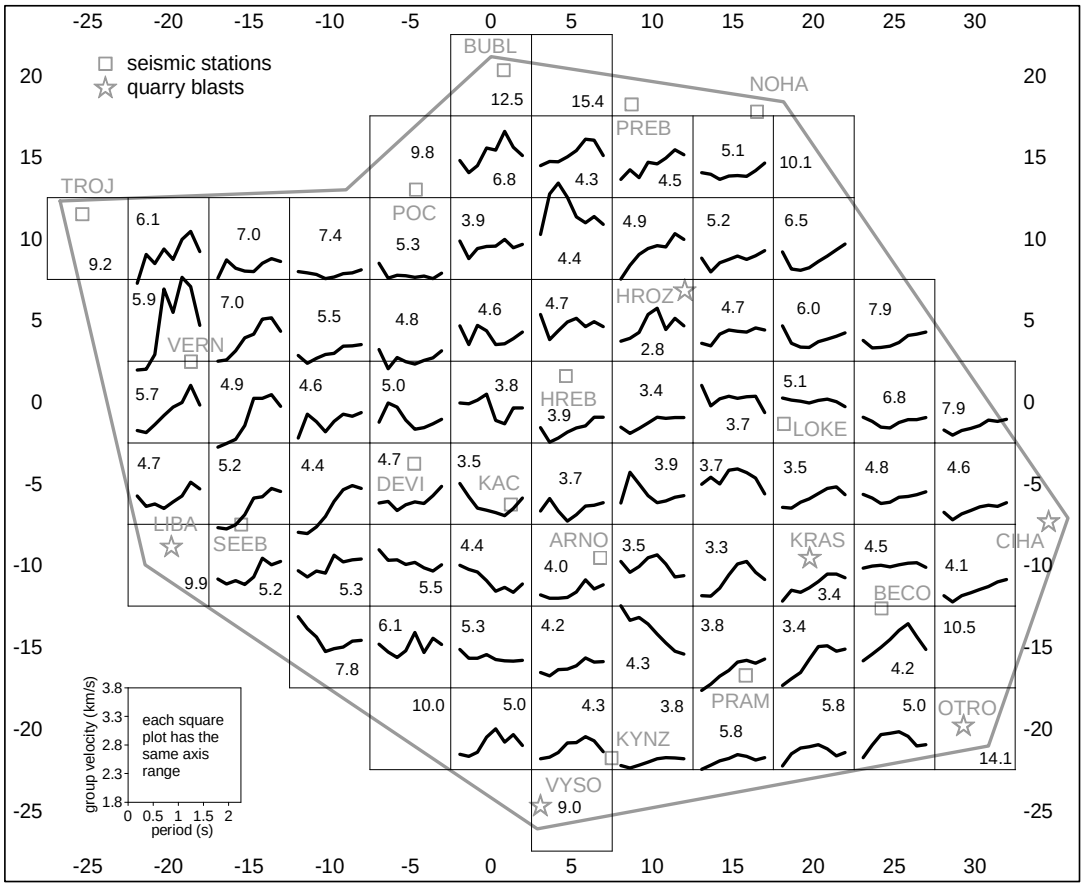

Fig. 6 Local dispersion curves corresponding to individual grid nodes (Fig. 2) presented in the Cartesian coordinate system. The nodes are to be imagined in the centre of each square plot. Each of the 79 plots has the same ranges of both axes. Studied area border is shown as well as the location of the stations (squares) and blasts (stars). The number in each plot gives the size of the averaging area in km for corresponding grid node and for period T = 0.5 s. Curves for nodes with averaging area size grater than 9.0 km are discarded.

depths of our model in comparison with the surface covered by more uniform sediments and disintegrated metamorphosed rocks. So, as a conclusion, we have to state, that less perturbed results for longer periods are given by limitations of the method and worse resolution ability of these wavelengths and that it does not necessarily mean that the surface structures are more heterogeneous than the deeper ones.

In all the map figures we depict a sketch of main geological features; they are described in the legend in Fig. 2. The most important features are two sedimentary basins, but our tomography does reveal only slight evidence of the smaller Sokolov basin (Fig. 2) as implies from lower velocity anomaly which is seen in the maps for periods of 0.25 to 1.0 s almost in the middle of the region of interest. Both basins are too shallow to be seen clearly even by the shortest periods and the Cheb basin (Fig. 2) produce even higher velocity anomaly for short periods. The basins are encircled by metamorphosed rocks and the velocity variations in them are rather random. The geological composition would probably not be the main phenomenon influencing the seismic velocities; the complicated fault system of the region and consequential surface wave multipathing and reflection may play a more important role in the scattered dispersion measurement.

The feature which we would like to emphasize is the direction of velocity anomalies. In case of shorter period maps (0.25 – 0.75 s) we see both high and low group velocity anomalies elongated in the southwest – northeast direction. On the other hand, in case of longer periods (1.25 – 2.0 s) we see a perpendicular direction – the anomalies are placed predominantly in the northwest – southeast direction. These are two main directions of complicated fault system in the Western Bohemia region. Southwest – northeast direction belongs to the Eger rift fault system and the perpendicular northwest – southeast direction follows the Mariánské Lázně fault. In the WB region, both fault systems meet each other.

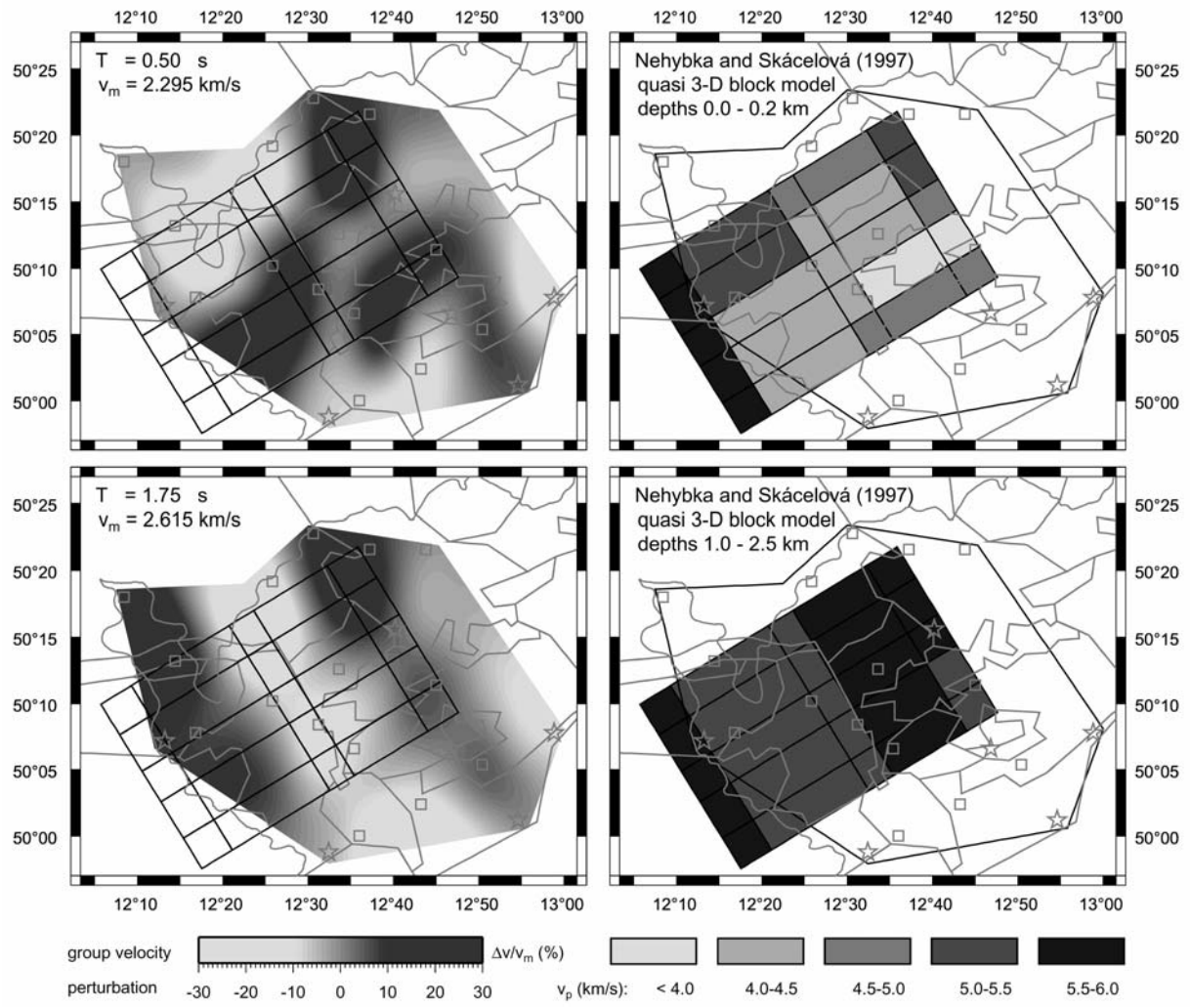

Fig. 7 Comparison of 2-D tomography maps for periods 0.5 and 1.75 s (the same as in Fig. 5) with the quasi 3-D block models of Nehybka and Skácelová (1997) for the depths of 0.0 – 0.2 km and 1.0 – 2.5 km respectively. Block edges are imagined in the left maps and tomography map borders in the right ones for better comparison.

We compare our velocity distribution with the results of Nehybka and Skácelová (1997). Their work is one of the few studies which deal with comparable depths and comparable geographical area, however, with body waves only. They used several 2-D refraction profiles to construct quasi 3-D block model of 125 blocks (5x5x5) of constant velocity. Their model covers only limited part the region of our interest and it reaches from surface to the depth of 4.5 km. Nehybka and Skácelová (1997) present only P wave velocity and we choose two layers from their results. Murphy and Shah (1988) give the relation

$$T = \frac{2.3H}{\overline{\beta}},$$

where T is the period of the group velocity in seconds, H is the depth to the significant discontinuity in kilometers, and $\overline{\beta}$ is the average shear wave velocity above this discontinuity in km/s. Since the shear wave velocities of the uppermost hundreds of meters in the WB region have the average value around 2.3 km/s (it is given by the limit of the group velocity for the shortest periods), a simple relation between the period of the wave and the depth of penetration is used: the period of the wave in seconds corresponds approximately to the depth in kilometers. We used this approach to compare our group velocity maps with the v_p distribution with depth. The 0.25 s group velocity tomography map is compared with 25-block map for the depth range 0.0-0.2 km of the model of Nehybka and Skácelová (1997) and our 1.75 s group velocity map is compared with their block velocity distribution in depths 1.0-2.5 km, see Fig. 7.

On the left panels of the Fig. 7 we present the same group velocity perturbation maps as in colored Fig. 5. We sketch the block edges in our map for better comparison. On the right panels we show the results of Nehybka and Skácelová (1997) with the

border of our tomography maps added. Nehybka and Skácelová (1997) set their block edges in the direction of predominant faults of the WB region. Even we are conscious of the comparison limitations of distributions of v_p and group velocity, we can make some qualitative conclusions. Both compared pairs show the same general directions of velocity anomalies. The 0.5 s and 0.0-0.2 km models show anomalies elongated in the southwest – northeast direction. Anomalies in both models tent to be more north – south directed than it is delineated by block edges. Low velocity anomaly in the center of our map is located more to the east than it is shown in the model of Nehybka and Skácelová. Similarly, the 1.75 s and 1.0-2.5 km models present anomalies in the predominant northwest – southeast direction. In this case they are elongated exactly along the block edges of v_p model. There are two low and two high velocity anomalies in the model of Nehybka and Skácelová and we have also found two pairs of anomalies in the same configuration. And again, our anomalies are shifted to the northeast in comparison with the v_p anomalies. The range of v_p velocities in the 0.0-0.2 km model is from 4.0 to 6.0 km/s, what presents distribution with perturbations 5.0 km/s ± 20%. Our models concern group velocities, which are sensitive more to the shear wave velocities, but the range of perturbation is in similar order of ± 25%, as clearly seen in colored Fig. 5. The 1.0-2.5 km model show smaller amount of perturbation of v_p from 5.0 to 6.0 km/s and our 1.75 s model is also smoother – the main anomalies in the center of the image range in order ± 15%. As we have already stated, this smoothness does not have necessarily structural consequences – it is influenced predominantly by worse resolution of the methods in greater depths. We may conclude that the main features and general properties of both models are the same. The direction of fault system is clearly visible in both studies and the correlation with geological composition is not found in either of them.

The high heterogeneity of the WB region may imply for more complicated surface wave propagation paths then assumed in our ray tomography. Anisotropy plays an important role as well but for its determination Love wave tomography would be needed. A surface topography of the region has an ability to influence the scattering of the dispersion measurement.

Better insight of the region's diversity may be seen in Fig. 6. If we look at the western part of our area of interest, around the node <-15,0>, we see dispersion curves with steep slope and wide range of velocities. As we go to the east, the slope of the curves becomes smaller. In the middle of the studied area around the node <+5,-5> there is almost no dispersion pronounced in the given period range. The same feature can be seen also in the northwest part around the node <-10,+5>. In the area of <+15,-5> the dispersions show even slower velocities for longer periods as well as it result in the southeastern and northern parts. Some of the dispersions around the border of our area are a bit scattered. Since the averaging areas are larger and hence the resolution is worse near the edges of the map, the information contained in these dispersions is less credible. Curves for nodes with averaging area size grater than 9.0 km are discarded.

These changes in dispersion curve slopes provide us with information about the vertical heterogeneity of different parts of the WB region. Detailed inversion of each of the local dispersion for S-wave velocity distribution with depth is needed in future studies.

ACKNOWLEDGEMENTS

This research was supported by grants No. A300460602 and No. A300460705 of the Grant Agency of the Academy of Sciences of the Czech Republic, by grant No. 205/06/1780 of the Czech Science Foundation and by Institute research plans No. A VOZ30460519 and No. MSM0021620860. We are grateful to prof. Tatiana B. Yanovskaya for providing her programs for surface wave tomography and for useful advice how to use them. Two of the figures are illustrated using Generic Mapping Tools by Wessel and Smith (1998).

REFERENCES

Beránek, B., Mayerová, M., Zounková, M., Guterch, A., Materzok, R. and Pajchel, J.: 1973, Results of deep seismic sounding along international profile VII in Czechoslovakia and Poland, Stud. Geophys. Geod., 17, 205-217.

Bourova, E., Kassaras, I., Pedersen, H. A., Yanovskaya, T., Hatzfeld, D. and Kiratzi, A.: 2005, Constraints on absolute S velocities beneath the Aegean Sea from surface wave analysis, Geophys. J. Int., 160, 1006-1019.

Brož, M.: 2000, Detection of the origin time and seismic ground motion of quarry blasts, Acta Montana, series A, 16 (118), 17-24.

Cara, M.: 1973, Filtering of dispersed wavetrains, Geophys. J. R. Astr. Soc., 33, 65-80.

Ditmar, P. G. and Yanovskaya, T. B.: 1987, An extension of the Backus-Gilbert technique for estimating lateral variations of surface wave velocities, Izvestia AN SSSR, Fizika Zemli, 6, 30-40, (in Russian).

Dziewonski, A., Bloch, S. and Landisman, M.: 1969, A technique for the analysis of transient seismic signals, Bull. Seism. Soc. Am., 59, 427-444.

Fischer, T. and Horálek, J.: 2003, Space-time distribution of earthquake swarms in the principal focal zone of the NW Bohemia/Vogtland seismoactive region: Period 1985 – 2001, J. Geodyn., 32 (1-2), 125-144.

Geissler, W. H.: 2005, Seismic and petrological investigations of the lithosphere in the swarm-earthquake and CO_2 degassing region Vogtland/NW-Bohemia, PhD thesis, scientific technical report STR05/06, GeoForschungsZentrum Potsdam, Potsdam, 150.

Grad, M., Špičák, A., Keller, G. R., Guterch, A., Brož, M., Hegedüs, E. and Working Group: 2003, SUDETES

2003 seismic experiment, Stud. Geophys. Geod., 47, 681-689.

Guterch, A., Grad, M., Keller, G. R., Posgay, K., Vozár, J., Špičák, A., Brückl, E., Hajnal, Z., Thybo, H., Selvi, O. and CELEBRATION 2000 Experiment Team: 2003, CELEBRATION 2000 seismic experiment, Stud. Geophys. Geod., 47, 659-669.

Heuer, B., Kämpf, H., Kind, R. and Geissler, W. H.: 2007, Seismic evidence for whole lithosphere separation between Saxothuringian and Moldanubian tectonic units in central Europe, Geophys. Res. Lett., 34, L09304, doi: 10.1029/2006GL029188.

Hrubcová P., Środa P., Špičák A., Guterch A., Grad M., Keller G. R., Brueckl E., and Thybo H.: 2005, Crustal and uppermost mantle structure of the Bohemian Massif based on CELEBRATION 2000 data, J. Geophys. Res., 110, B11305.

Janský, J. and Novotný, O.: 1997, Reinterpretation of the travel times of P waves generated by quarry blasts in Western Bohemia, Acta Montana, series A, No. 11 (104), 35-48.

Janský, J., Horálek, J., Málek, J. and Boušková, A.: 2000, Homogeneous velocity models of the West Bohemian swarm region obtained by grid search, Stud. Geophys. Geod., 44, 158-174.

Kolínský, P., 2004: Surface wave dispersion curves of Eurasian earthquakes: the SVAL Program, Acta Geodyn. Geomater., Vol. 1, No. 2 (134), 165-185.

Kolínský, P. and Brokešová, J.: 2007, The Western Bohemia uppermost crust shear wave velocities from Love wave dispersion, Journal of Seismology, 11, 101-120.

Kolínský, P. and Málek, J.: 2007, Shear wave crustal velocity model of the western Bohemian Massif from Love wave phase velocity dispersion, Geophys. J. Int., submitted.

Levshin, A., Pisarenko, V.F. and Pogrebinsky, G.A.: 1972, On a frequency-time analysis of oscillations, Ann. Geophys., Vol. 28, No. 2, 211-218.

Levshin, A.L., Yanovskaya, T.B., Lander, A.V., Bukchin, B.G., Barmin, M.P., Ratnikova, L.I. and Its, E.N.: 1989, Interpretation of surface wave observations – frequency-time analysis, In: Keilis-Borok, V. I. (ed.): Seismic Surface Waves in a Laterally Inhomogeneous Earth, Kluwer Academic Publishers, Dordrecht/Boston/London, 153–163.

Málek, J., Janský, J. and Horálek, J.: 2000, Layered velocity models of the Western Bohemia Region, Stud. Geophys. Geod., 44, 475-490.

Málek, J., Janský, J., Novotný, O. and Rössler, D.: 2004, Vertically inhomogeneous models of the upper crustal structure in the West-Bohemian seismoactive region inferred from the CELEBRATION 2000 refraction data, Stud. Geophys. Geod., 48, 709-730.

Málek, J. and Žanda, L.: 2004, Seismic effects of the quarry blasts on the territory of Bohemia, Acta Geodyn. Geomater., Vol. 1, No. 2 (134), 291-302.

Málek, J., Horálek, J. and Janský, J.: 2005, One-dimensional qP-Wave Velocity Model of the Upper Crust for the West Bohemia/Vogtland Earthquake Swarm Region, Stud. Geophys. Geod., 49, 501-524.

Malinowski, M.: 2005, Analysis of short-period rayleigh waves recorded in the Bohemian Massif area during CELEBRATION 2000 experiment, Stud. Geophys. Geod., 49, 485-500.

Mlčoch, B., Schulmann, K., Šrámek, J., Manová, M., Pokorný, L., Fiala, J. and Vejnar, Z.: 1997, Geological interpretation of major regional units – The Saxothuringian Zone, in: Vrána, S. and Štědrá, V. (eds.): Geological Model of Western Bohemia Related to the KTB Borehole in Germany, Czech Geological Survey, Prague, 51-60.

Murphy, J.R. and Shan, H.K.: 1988, An analysis of the effects of site geology on the characteristics of near-field rayleigh waves, Bull. Seism. Soc. Am, Vol. 78, No. 1, 64–82.

Nehybka, V. and Skácelová, Z.: 1997, Seismological study of the Kraslice/Vogtland-Oberpfalz region, in: Vrána, S. and Štědrá, V. (eds.): Geological Model of Western Bohemia Related to the KTB Borehole in Germany, Czech Geological Survey, Prague, 186-190.

Novotný, M.: 1997, The ray interpretation of DSS data from the VI/70 seismic transect across the Bohemian Massif, in: Vrána, S. and Štědrá, V. (eds): Geological Model of Western Bohemia Related to the KTB Borehole in Germany, Czech Geological Survey, Prague, 131-139.

Novotný, O., Proskuryakova, T.A., Shilov and A.V.: 1995, Dispersion of rayleigh waves along the Prague-Warsaw profile, Stud. Geophys. Geod., 39, 138-147.

Novotný, O.. 1996, A preliminary seismic model for the region of the West-Bohemian earthquake swarms, Stud. Geophys. Geod., 40, 353-366.

Novotný, O., Grad, M., Lund, C.E. and Urban, L.: 1997, Verification of the lithospheric structure along profile Uppsala-Prague using surface wave disperison, Stud. Geophys. Geod., 41, 15-28.

Novotný, O., Janský, J. and Málek, J.: 2004, Some aspects of the application of the Wiechert-Herglotz method to refraction data from Western Bohemia, Acta Geodyn. Geomater., Vol. 1, No. 2 (134), 157-164.

Plešinger, A., Neunhöfer, H. and Wielandt, E.: 1991, Crust and upper mantle structure of the Bohemian Massif from the dispersion of seismic surface waves, Stud. Geophys. Geod., 35, 184-195.

Plomerová, J., Babuška, V., Janatková, Z. and Lokajíček, T.: 1987, Directional dependence of seismic waves propagation of the 1985–86 earthquake swarm in Western Bohemia, in: Procházková, D. (ed.): Earthquake Swarm 1985/86 in Western Bohemia - Proceedings of Workshop in Mariánské Lázně, Czechoslovak Academy of Sciences, Geophysical Institute, Prague, 197-204.

Raykova, R. and Nikolova, S.: 2007, Tomography and velocity structure of the crust and uppermost mantle in Southeastern Europe obtained from surface wave analysis, Stud. Geophys. Geod. 51, 165-184.

Růžek, B., Hrubcová, P., Novotný, M., Špičák, A. and Karousová, O.: 2007, Inversion of travel times obtained during active seismic refraction experiments CELEBRATION 2000, ALP 2002 AND SUDETES 2003, Stud. Geophys. Geod., 51, 141-164.

Špičák, A., Horálek, J., Boušková, A., Tomek, Č. and Vaněk, J.: 1999, Magma intrusions and earthquake swarm occurrence in the western part of the Bohemian Massif, Stud. Geophys. Geod., 43, 87-106.

Yanovskaya, T.B. and Ditmar, P.G.: 1990, Smoothness criteria in surface wave tomography, Geophys. J. Int., 102, 63-72.

Yanovskaya, T.B., Kizima, E.S. and Antonova, L.M.: 1998, Structure of the Black Sea and adjoining regions from surface wave data, Journal of Seismology, 2, 303-316.

Yanovskaya, T.B., Antonova, L.M. and Kozhevnikov, V.M.: 2000, Lateral variations of the upper mantle structure in Eurasia from group velocities of surface waves, Physics of the Earth and Planetary Interiors, 122, 19-32.

Yanovskaya, T.B. and Kozhevnikov, V.M.: 2003, 3D S-wave velocity pattern in the upper mantle beneath the continent of Asia from rayleigh wave data, Physics of the Earth and Planetary Interiors, 138, 263-278.

Wessel, P., and Smith, W.H.F.: 1998, New, improved version of generic mapping tools released, Eos Trans. AGU, 79 (47), 579.

Wielandt, E., Sigg, A., Plešinger, A. and Horálek, J.: 1987, Deep structure of the Bohemian Massif from phase velocities of rayleigh and Love waves, Stud. Geophys. Geod., 31, 1-7.

Wilde-Piórko, M., Saul, J. and Grad, M.: 2005, Differences in the crustal and uppermost mantle structure of the Bohemian Massif from teleseismic receiver functions, Stud. Geophys. Geod., 49, 85-107.